International Journal of Engineering and Technical Research (IJETR)
ISSN: 2321-0869 (O) 2454-4698 (P), Volume-6, Issue-3, November 2016

Removal of fluorescence and shot noises in Raman spectra of biological samples using morphological and moving averages filters

Claudia C. Soberón-Celedón, J. Rafael Molina-Contreras, Claudio Frausto-Reyes, Juan Carlos Zenteno-Ruiz

***Abstract*— in this paper we show that it is possible to drastically reduce the fluorescence and shot noises in Raman spectra by means of a mathematical method which uses morphological and moving averages filters. Proved on biological materials, simulations show that after the application of the morphological and the moving average filters on the raw Raman data, the line shape is basically free of fluorescence background, free of shot noise and that the peaks keep their original characteristics as position, intensity, area and relative intensity among peaks. In addition to this, the low intensity peaks masked by the mentioned noises are defined after the operations. The noise removal method reported in this paper may have an immediate application in improving the spectroscopic processes for food quality assurance and for the screening of metabolites in human samples.**

***Index Terms*— near infrared Raman spectroscopy, noise removal, morphological filter, moving averages filter, biological samples**

I. INTRODUCTION

Raman spectroscopy has proven to be an extremely capable tool to characterize semiconductors [1] and identify crystal pigments [2-7] among other possibilities [8-10]. The small signal obtained in a standard Raman measurement however, diminishes not only the efficiency of the technique, but it can become in a major drawback in the data analysis. Background noises as shot and those due to the instruments may limit the detection of the Raman signal too as fluorescence does. The case of fluorescence; which is the most common source of the background noise in Raman spectroscopy, is very significant by consider that it can be intrinsic to the studied sample. As the fluorescence is usually some orders of magnitude higher than the Raman signal, it could easily compromise the data analysis if it masks some of the characteristic bands associated to the material. Due to this, the presence of fluorescence in a Raman spectrum generally reduces the effective observation of the useful signal. Both shot and fluorescence noises urge then a reduction of their intensities as a need for a clear identification and later characterization of the bands of the studied samples by Raman spectroscopy. This is of paramount importance when the Raman spectroscopy is applied to study biomolecules samples which intrinsic shot and fluorescence noises may mask the useful signal. Mathematical and instrumentation methods have been proposed in order to eliminate the fluorescence level; but for our knowledge, this has not been done to eliminate the shot noise; and less in the same proposal.

All morphological operations are basically the result of one or more operations of union or intersection among others between two sets of data X, Y, which pertain to a Z space. In the operation between two sets of data X and Y for example, one of the sets (Y for instance) is designated as the structuring element, which will operate with the X set. Due to this, the structuring element is shifted through to the Z space. As a result, the operation transforms the data of X into another set. The transformation results help to visualize unique geometric structures in the original data set X using the structuring element Y in the study of the data related to any sample. The shape of Y is chosen a priori according with the morphology of the set to be transformed and with the special structures which will be extracted. This way, mathematical morphology has been used lately as a nonlinear processing technique mainly in digital image processing. The only requirement for its application, involves the use of sets of data and their properties [11-13]. In any case, the mathematical morphology is based on a classical theory [14].

Erosion and dilation are the most basic morphological operations and they are the basis of any morphological transformation. The expression in one dimension for the erosion of a function $f(x)$ by a structuring element Y is defined as the minimum value of the function in the window determined by the structuring element centered at *x*. The expression in one dimension for the dilation of a function $f(x)$ by a structuring element Y on the other hand, is defined as the maximum value of the function in the window determined by the structuring element also centered at *x*. The erosion and dilation functions are transformations with no inverse, this way; the original signal cannot be recovered from them. The original signal however can be approximated using erosion followed by dilation with the same structuring element. This morphological operation is called opening. A dilation followed by erosion is a morphological closing operation. Both opening and closing are the basic morphological operations to remove noise. Opening removes small features while closing removes small holes into which a specific structural element can fit. The opening of a function is obtained by the erosion of the function by Y following by the dilation of the resulting function after the erosion and is described mathematically as

Claudia C. Soberón-Celedón, Posgrado, Instituto Tecnológico de Aguascalientes/ Aguascalientes, México, +52 (449) 910 50 02

J, Rafael Molina-Contreras, Eléctrica-Electrónica, Instituto Tecnológico de Aguascalientes/ Aguascalientes, México, +52 (449) 910 50 02

Claudio Frausto-Reyes, Fotónica, Centro de Investigaciones en Óptica, Unidad Aguascalientes, Aguascalientes, México, +52 (449) 442 81 24.

Juan Carlos Zenteno-Ruiz, Genética, Instituto de Oftalmología Conde de Valenciana, Ciudad de México, México.

$$O_Y f(x) = \delta_Y(\varepsilon_Y f(x)) \quad (1).$$

Where $\varepsilon_Y f(x)$ and $\delta_Y f(x)$ are the erosion and dilation functions respectively. The result is a nonlinear smoothing of the signal by removing the positive peaks narrower than the structuring element. That is, the opening always takes values lower than the original set and can approximate the baseline of a spectrum. A morphological operation called top-hat transformation allows determining the structures eliminated by the opening operation. Mathematically it can be described like this

$$thf(x) = f(x) - O_Y f(x) \quad (2).$$

Where $thf(x)$ is the top-hat transformation; $f(x)$ is the function related to the X data set and $O_Y f(x)$ is the opening function. The top-hat operation can be used to obtain a baseline-free spectrum.

Moving averages is the underlying concept behind the trading indicators and it has remained unaltered for more than a half of century [15-18]. The development in this field has consisted basically in proposing new ad-hoc rules and using more elaborate types of moving averages in the existing rules because it still gives reliable results to the present day. Working with past and current market prices, trading volume and other public information, the moving average technique is widely used to predict market prices. The performance of any moving average depends exclusively on the shape of the weighting function N. A N-interval Moving Average (MA) at interval-end f is computed as:

$$MAf(N) = \frac{(n_0, n_1, \ldots n_f)}{N} \quad (3).$$

Where $n_0, n_1, \ldots n_f$ are the most recent observations of the closed interval; N is the weighting function and f is the interval-end.

In this paper we report on the results of the application of a mathematical two steps method (implemented in a homemade program which uses morphological and moving average operations together) in order to remove the fluorescence and shot noises from the Raman spectra of biological samples. Our results show that the method not only leaves unchanged the characteristics of the line shape of the Raman signal as position, intensity, area and relative intensity among peaks position; but drastically reduces the fluorescence and the characteristic ripple of the shot noise. The results reported in this work show the utility of both morphological and moving average filters together in the removing of intrinsic noises of biological samples. The noise removal method reported in this paper may have an immediate application in improving the spectroscopic processes for food quality assurance and for the screening of metabolites in human samples.

II. EXPERIMENTAL

The samples used in this work were: a sample of fresh carrot, a commercial tomato sauce, a gray human hair, and a sample of human serum. In the three first cases, the samples were taken without any preparation. The sample of the human serum was obtained from a patient clinical diagnosed with corneal ulcer treated in the Institute of Ophthalmology Conde de Valenciana, México City, México. Upon obtaining the blood sample, it was centrifuged at 3500 rpm for 10 minutes. After this, the sample was frozen in an ultra-freezer at -50°C for preservation. For the Raman measurements, the sample was passively thawed at room temperature. The Raman spectra of the samples were measured using a micro-Raman system (Ranishaw1000B) with a back scattering geometry [19] with a 600 lines/mm grating and a CCD camera (RemCam1024×256 pixels). The wavelength used in the system is of 830 nm and its laser beam with a spot-size of about 2mm was focused onto the sample with a 50×objective of a Leica (DMLM) microscope. To reduce the intrinsic noises of fluorescence and shot from the raw spectra, all data were treated with a home-made program which uses the morphological and moving average operations indicated in the second and third paragraphs of the results and discussions of this paper. In all the cases, the home-made program was run on the MatLab platform. Prior to the measurement, the Raman system was calibrated with the 520 cm^{-1} Raman peak of a silicon semiconductor. All signals were taken under the same experimental conditions with an exposure of 60 seconds.

III. RESULTS AND DISCUSSION

As it was previously stated, the small signal obtained in a Raman standard measurement is basically on a fluorescence signal usually some orders of magnitude higher than the Raman signal. Due to this, the useful signal may easily be mask for the fluorescence. This in turn makes the characterization a very complicated task. This is worst if the Raman signal has an additional high content of other noises: say shot, atmospheric, etc. This is the reason why any new method to clean the signal is of paramount importance. With a useful signal free of noises the data analysis is highly simplified. And in any sense, a clear identification of the characteristic bands of a material will increase the effectiveness of the technique itself to apply it for example in improving the spectroscopic processes for food quality assurance and the screening of metabolites in human sera samples in a first approach.

The foundations of the mathematical filters used in this work for the suppression of fluorescence and shot noises in the Raman spectra of biological samples uses an averages opening operation as

$$O'f(x) = \frac{\delta[O_Y f(x)] + \varepsilon[O_Y f(x)]}{2} \quad (4);$$

This gives a closer baseline in the regions where there are Raman bands. After that, the filter uses an expression like

$$O_{bp} f(x) = \min[O'f(x), O_Y f(x)] \quad (5),$$

To obtain the best approach of the baseline; the baseline is removed by applying the top-hat transformation which gives the correction for the opening operation as it was proved in reference [20].

For the removal of the shot noise we employed a moving average operation like

$$MA = \frac{\sum(\text{n most recent data values})}{N} \quad (6).$$

In equation (6), N is the basis for the moving averages. Although there is no specific rule on how to select the basis of the moving average N, it is recommended a large N when the behavior of the data is relatively stable over time. Conversely, if the variable shows changing patterns; it is advisable to use a small N value. In practice, values for N between 2 to10 are normal. In this work the N value was equal to 5. These operations were implemented in the mentioned homemade program for simulation.

Just to compare and to show the effect of the mentioned filters on the raw data of our experiment, we start our discussion with the Raman spectrum of a carrot sample. Figure 1(a) shows the raw Raman spectrum as was obtained following the directives indicating in experimental section. Figure 1(b), shows the effect of the morphological filter on the raw data of the Raman spectrum. Figure 1(c), shows the effect of the moving averages filter on the results obtained after the morphological filter on the original data of the Raman spectrum of the carrot sample.

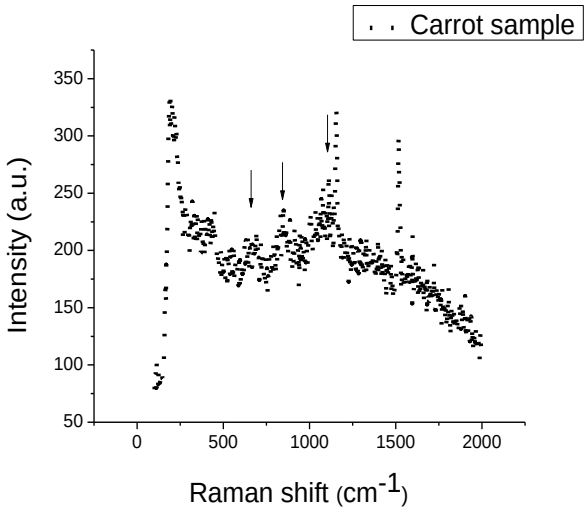

Fig. 1(a) Raw Raman spectrum of a carrot sample as was obtained following the directives indicating in experimental section.

In Figure 1(a) as it can be seen, the Raman signal is drastically affected by a background of a lower frequency signal of fluorescence with a very high level of intensity compared with the Raman signal; and a very high frequency shot noise. It is clear in this figure, that the fluorescence level almost masks the signal of interest. It also hinders the proper characterization of the sample bands. Due to this, the maximums of the three wide bands suggested in the line shape of figure 1 (a) cannot be visualized accurately. The noise level in the region between 1100 and 1550 cm^{-1} on the other hand could avoid a clear identification of the two higher peaks located in such region.

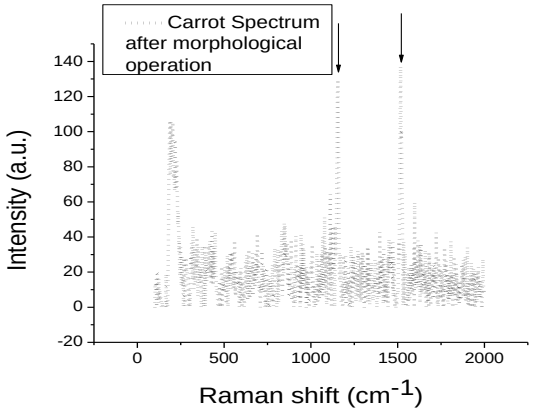

Fig. 1(b) Raman spectrum after the morphological filter on the raw data of a carrot sample obtained as indicated in the experimental section.

In Figure 1(b) as it can be seen, the fluorescence has been reduced several orders of magnitude. Because of this, the shot noise is much more noticeable and their intensities along the entire region, as it can be seen, completely mask even the three wide bands suggested in the raw Raman spectrum. Particularly, the noise intensity between 1100 and 1550 cm^{-1} make harder the identification of the two higher peaks located in such region; however, such peaks still keep the same position. The results in figure 1(b) show that the morphological filter is not enough to suppress the unwanted signals in the raw data. This is particularly true in the study of biological samples as the one discussed in this section, which has a complicated intrinsic noise family.

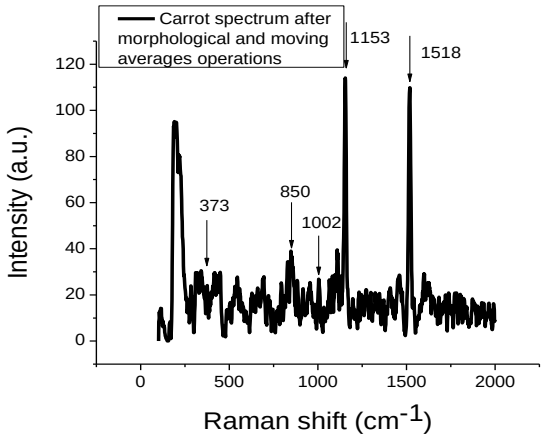

Fig.1(c) Raman spectrum after the moving averages filter on the results obtained after the morphological filter on the raw Raman spectrum of carrot sample.

In Figure 1(c) as it can be seen, the application of the moving averages filter on the data obtained after the morphological filter; reduces drastically the high content of the shot noise. The treatment of the signal after the morphological filter with a moving averages operation as the one used in this work leaves, as it can be seen in figure 1(c), the Raman signal of the biological sample almost without noise. After the moving averages filter it is clear that the higher peaks indicated with arrows in figure 1 (b) are due to the material; and that there were not three wide bands as indicated in figure 1 (a) but five due to the material in the region between 305 and 1000 cm^{-1}. Figure 1(c) also shows a

triplet of low intensity peaks around the peak located around 1518 cm^{-1}, which were completely masked even after the morphological filter. In conclusion, the moving averages filter has uncovered the Raman signal of the carrot sample which mainly includes the five wide bands in the region between 305 and 1000 cm^{-1} and the higher peaks located between 1100 and 1550 cm^{-1}. After the morphological and moving averages filters on the raw Raman data it is easy to identify in figure 1(c) the bands due to carotene located at 1153 and 1518 cm^{-1} which are in agreement with reference [21]. Possibly also, the lycopene located at 1002 cm^{-1} in agreement with reference [23] and pectin in accordance with [24] located at 374, and 852 cm^{-1}. These results clearly show that the combination of the morphological and moving average operations applied to the raw Raman data of a carrot sample step by step, is a reliable method for the suppression of fluorescence and shot noises in the Raman signal of biological samples; taking into account that such operations keep the position, area, intensity, and relative intensity of the sample Raman peaks. Our results not only suggest that the mayor drawback of the Raman signal, the fluorescence, can be eliminated from the raw spectra obtained on biological samples, but that the shot noise and those due to the instruments; which also may limit the use of the technique, can be suppressed too in an automatic two steps procedure. This in turns becomes a mayor advantage in the study of biological materials. Our results show that the noise removal method reported in this paper, may have an immediate application in improving the spectroscopic processes for food quality assurance.

In order to complete our analysis and to prove the efficiency of the suppression filters used in this work, we measured the Raman spectra of a commercial ketchup sauce; a human grey hair and a human serum samples. Figure 2 shows the raw Raman spectrum of the commercial ketchup sauce with filled black dots; the data after the morphological filter with empty circles; and the data after the morphological and moving average filters with a solid line. In this figure as it can be seen, we have again a lower frequency signal of fluorescence with a very strong level of intensity compared with the Raman signal. The logic consequence of such high offset is the masking of the structure of the material in the spectrum. Under these circumstances, is easy to see the necessity of an urgent treatment to reduce the fluorescence at least. In this case, the results of the application of the first step of our method to suppress the fluorescence level in the raw commercial ketchup sauce spectrum are seen in figure 2. The empty circles in this figure show that after the morphological filter, the strong fluorescence level has been reduced again several orders of magnitude; and its consequences are clearly shown with the appearance of the characteristic structure of the spectrum. The results of the morphological filter however, still show the presence of shot noise. This is particularly evident in the region between 750 and 1100 cm^{-1}. Due to this, it was applied again the moving averages filter to the results obtained after the morphological filter. Figure 2 show with a solid line the results after the morphological and moving averages filters on the raw commercial ketchup sauce spectrum. Our results show again that after the morphological and the moving average filters, the strong fluorescence level and the shot noise have been suppressed in a way that the characteristic structure of the spectrum is clearly seen. The solid line in this figure clearly show the Raman bands of the tomato puree related to the lycopene at 1508 and 1003 cm^{-1}; the one related to β-carotene at 1155 cm^{-1} [21]; and possible also the peak related to glucose at 417cm^{-1} [22]. These results confirm that our noise removal method may have an immediate application in improving the spectroscopic processes for food quality assurance.

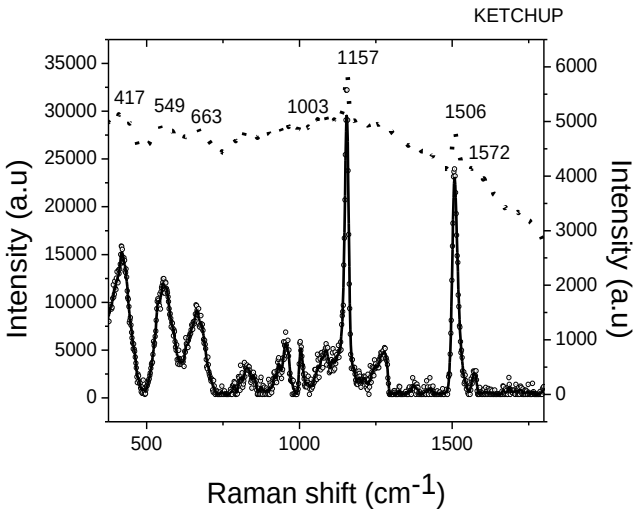

Fig. 2 Raw Raman spectrum of a commercial ketchup sauce (black dots). Raman spectrum of a commercial ketchup sauce, after the morphological operations (open circles). Raman spectrum after the moving averages operation on the results obtained after the morphological operations on the raw Raman spectrum of a commercial ketchup sauce (solid line).

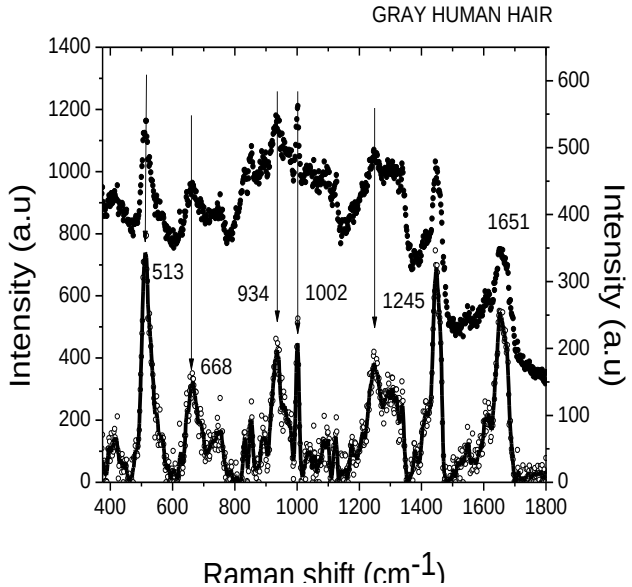

Fig. 3 Raw Raman spectrum of a gray human hair sample (black dots). Raman spectrum of a gray human hair sample, after the morphological operations (open circles). Raman spectrum after the moving averages operation on the results obtained after the morphological operations on the raw Raman spectrum of a gray human hair sample (solid line).

Figure 3 shows the raw Raman spectrum of a gray human hair with filled black dots; the data after the morphological

filter with empty circles; and the data after the morphological and moving average filters with a solid line. In this case, as shown in the line shape of the filled black dots; although the fluorescence level allows seeing the structure of the material, there is still a problem for an appropriate characterization. This is due to the so poor resolution of such line shape. This is a particular problem in the region centered at 1000 cm^{-1} where the bands are not clearly resolved on the picture of the raw data. This is evident after the application of the morphological filter to the raw data to suppress the fluorescence level. The effect of the morphological filter on the raw data as it can be seen, not only reduces drastically the fluorescence level, but leaves in sight a very sharp peak and an asymmetric band clearly defined in the region between the 900 and 1000 cm^{-1}.

Our results show again that the consequences of this filter, define completely the structure of the gray human hair spectrum. This effect also shows the invariance in the location of the peaks after the application of the morphological filter to the raw data, which is one of the mayor features of our method in the removing of undesirable noises from the useful signal. The shot noise however, still remains after the application of the morphological filter. This is particularly evident in the region between 600 and 1800 cm^{-1}, where the shot noise has a significant level and may become a problem for proper characterization. These results highlight again the need for the moving averages filter even in the cases where the morphological operations show the structure of the material. The solid line in figure 3 shows our results after the morphological and the moving average filters on the raw data of the gray human hair sample. This solid line shows the complexity of the gray human hair spectrum. In this solid line shape it is possible to identify the Cysteine at 513 and 668 cm^{-1}; the amide I at 934 and 1651 cm^{-1}; the amide III at 1245 cm^{-1} and the phenylalanine around 1002 cm^{-1}[25]. These results suggest that the application of the method may also be useful for the screening of the metabolites in samples of human origin.

In a first approach, the human serum complex structure can be divided into two regions: region A from 1500 to 600cm^{-1} and region B from 600 to 375cm^{-1}. Region A has a large number of Raman bands which can be assigned to fats, amino acids, primary metabolites, glucose and others [26-27]. This situation of a mix of analytes embedded in a matrix containing other components, which have their own signals and their bands spliced on each other; complicate the clear identification of a particular analyte in region A. Region B has a less influence of the other analytes mixed in the matrix and it contains the biggest plasma carbohydrate [28]. However, even with a virtually null influence of the other components of the mix, a high content of noises in the Raman signal is always a problem for a proper characterization.

Figure 4 shows the raw Raman spectrum of a human serum sample with filled black dots; the data after the morphological filter with empty circles; and the data after the morphological and moving average filters with a solid line. In this case, as shown in the line shape of the filled black dots; the fluorescence level completely masks the real structure of the human serum within region A. Such structure however, is completely exposed after the application of the morphological filter, leaving in view its complexity.

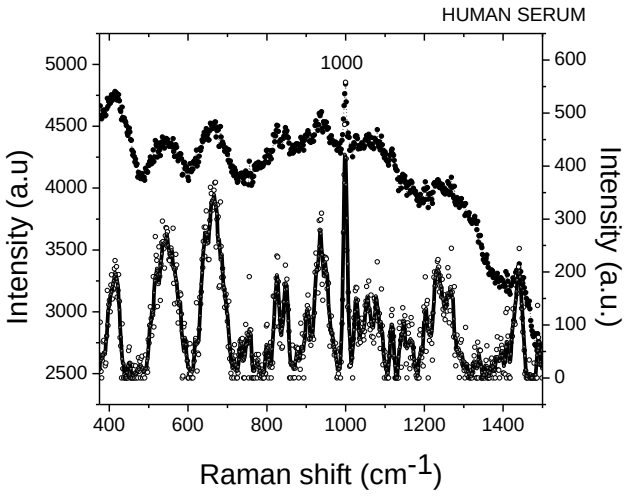

Fig. 4 Raw Raman spectrum of a human serum sample (black dots). Raman spectrum of a human serum sample, after the morphological operations (open circles). Raman spectrum after the moving averages operation on the results obtained after the morphological operations on the raw Raman spectrum of a human serum sample (solid line).

The effect of the morphological filter on the raw data as it can be seen in this case again, not only reduces the fluorescence level several orders of magnitude, but leaves in sight the very sharp peak related to the phenylalanine and some asymmetric bands split in doublets and triplets in the region between 700 and 1300 cm^{-1}. Our results also suggest in this case the invariance of the peaks form and positions with the application of the morphological filter to the raw data. Such filter however, as in the other cases described in previous paragraphs, leave the shot noise level in the whole domain of the studied region. These results again, highlight the need for the moving averages filter. The solid line in figure 4 shows our results after the morphological and the moving average filters on the raw data of a very complicated line shape as the one related to the human serum sample. In this solid line is easy to see that both regions A and B of the complex human serum spectrum have been revealed after the morphological and the moving averages filters. Such filters have left a line shape free of fluorescence background, free of noise and with its original line shape. These results are clearly remarkable in the great definition of the phenylalanine, which is located around 1000 cm^{-1} and characterize the human serum. Our results also suggest that after the human serum signal treatment with our method, the two peaks located in the region between 375 and 600 cm^{-1} may be become clear candidates for the glucose identification in human serum [22, 29] after the noise reduction. This a logical conclusion considering the less influence of the other analytes of serum the mix; and the clear definition obtained after the treatment of the signal with our method. This results confirm that our method maybe useful for the screening of metabolites in human samples.

IV. CONCLUSIONS

A two steps automated method to suppress the fluorescence and shot noises in the Raman spectra has been implemented in a homemade program and proved on biological materials

spectra. Based on morphological and moving averages operations, the method seems to be efficient. Simulations show that after the application of the morphological and the moving average operations on the raw Raman data, the line shape is free of fluorescence background, free of shot noise and that the peaks keep their original form such as position, area, intensity, and relative intensity among peaks. In the addition to this, the method can resolve the low intensity peaks which could be masked due to the fluorescence and the shot noises. Our results suggest that the method may have an immediate application in improving the spectroscopic processes for food quality assurance and for the screening of metabolites in human samples.

ACKNOWLEDGMENT

The authors are grateful to CONACYT, México for financial support.

REFERENCES

[1] J Rafael Molina Contreras, C Frausto-Reyes, C I Medel-Ruiz, H Pérez Ladrón de Guevara and C Medina-Gutiérrez, *J. Phys. D: Appl. Phys*. **46**, 245105, 2013, (4pp)
[2] F. Schulte, K.-W. Brzezinka, K. Lutzenberger, H. Stege, and U. Panne, *J. Raman Spectrosc*. **39**, 2008, 1445
[3] L. Burgio, R. J. H. Clark, V. S. F. Muralha, and T. Stanley, *J. Raman Spectrosc*. **39**, 2008,1482
[4] D. de Waal *J. Raman Spectrosc*. **38**, 2007, 956
[5] S. E. Jorge Villar, H. G. M. Edwards, J. Medina, and F. Rull Perez, *J. Raman Spectrosc*. **37**, 2006, 974
[6] R. Pérez-Pueyo, M. J. Soneira, and S. Ruiz-Moreno, *J. Raman Spectrosc*. **35**, 2004, 808
[7] M. Castanys, R. Pérez-Pueyo, M. J. Soneira, and S. Ruiz-Moreno, *J. Raman Spectrosc*. **37**, 2006 , 1003
[8] P. Matousek, E. R. C. Draper, A. E. Goodship, I. P. Clark, K. L. Ronayne, and A. W. Parker, *Appl. Spectrosc*. **60**, 2006 , 758
[9] M. F. Escoriza, J. M. VanBriesen, S. Stewart, and J. Maier, *Appl. Spectrosc*. **61**, 2007, 812
[10] Y. Liu, K. Chao, M. S. Kin, D. Tuschel, O. Olkhovyk, and R. J. Priore, *Appl. Spectrosc*. **63**, 2009, 477
[11] Z. Yu-qian, G. Wei-hua, C. Zhen-cheng, T. Jing-tian, and L. Ling-yun, *Proceedings of 27th Annual International Conference of the Engineering in Medicine and Biology Society*, 2005, 6492
[12] D. Ze-Feng, Y. Zhou-Ping, and X. You-Lun, *IEEE Signal Process. Lett*. **14**, 2007, 31
[13] C. Hao-Teng, L. Chih-Hong, and P. Tun-Wen, J, *Mol. Recognit*. **21**, 2008, 431
[14] A. A. Fraenkel, Y. Bar-Hillel, and A. Levy, Foundations of Set Theory, Elsevier Science Publishers, Noth Holland, 1984
[15] Hong, K. J. and Satchell, S, *Quantitative Finance*, **15** (9), 2015, 1471-1487
[16] Clare, A., Seaton, J., Smith, P. N., and Thomas, S, *Journal of Asset Management*, **14** (3), 2013, 182–194
[17] Kilgallen, T, *Journal of Wealth Management*, **15** (1), 2012, 82–100
[18] Gwilym, O., Clare, A., Seaton, J and Thomas, S, *Journal of Investing*, **19** (3), 2010, 80–91
[19] G. Turrel, M. Delhaye, P. Dhamelincourt, in: G. Turrel, *J. Corset (Eds.)*, 232 Raman Microscopy, Developments and Applications, Academic Press, 233, London, 1996, pp. 27–49
[20] Rosanna Perez Pueyo, Maria Jose Soneira and Sergio Ruiz-Moreno, *Applied Spectroscopy*, Volume **64**, Number 6, 2010, 595-600
[21] M. Baranska, H. Schulz, R. Baranski, T. Nothnagel y L. Christensen, *Journal of Agricultural and Food Chemistry*, vol. **53**, nº 17, 2005, pp. 6565-6571
[22] J. Gelder, K. Gussem, P. Vandenabeele and L. Moens, *Journal of Raman Spectroscopy*, vol. **38**, no. 9, 2007, pp. 1133-1147
[23] H. Ming-Ming, L. Wei-Long, Z. Zhi-Ren, Z. Wei y L. Ai-Hua, *Molecules*, vol. **16**, 2011, pp. 1973-1980
[24] D. o. F. Science, Available at: http://www.models.life.ku.dk/. [last acces: 04 02 2015].
[25] A. Kuzuhara, N. Fujiwara y T. Hori, *Biopolymers*, vol. **87**, nº 2-3, 2007, pp. 134-140
[26] Villanueva, A., Castro, J., Vazquez, S., Flores, A., Ortiz, C and Delgado, J. Raman spectroscopy of blood in-vitro. Optical Diagnostics and Sensing XII: Toward Point-of-Care Diagnostics; and Design and Performance Validation of Phantoms Used in Conjunction with Optical Measurement of Tissue IV, 2012, 8229. San Francisco, California, USA
[27] Feng, S., Chen, R., Lin, J., Pan, J., Chen, G., Li, Y, *Biosensors and bioelectronics* , **25** (11), 2010, 2414-2419
[28] Rhoades, R., and Bell, D, *Lippincott Williams and Wilkins*, Medical physiology : principles for clinical medicine, 2013, (4th ed.)
[29] J. Goral, *Current Topics in Biophysics*, vol. **16**, nº 1, 1990, pp. 33-47.

Claudia C. Soberón-Celedón Engineering PhD student, Glucose sera study using Raman spectroscopy, Serum glucose study around the skeletal vibration domain using Raman spectroscopy (internal communication), Signal Analysis, Apply Chemistry.

J. Rafael Molina Contreras Sciences PhD, Transversal acoustic modes in resonant Raman: CdTe surface roughness study, The self assembly of thymine at Au(110)/liquid interfaces, THz-time domain spectroscopy of (001) ZnSe, Reflectance Difference Spectroscopy, Raman Spectroscopy, THz time domain spectroscopy, Mexican National Researcher, Reflectance equation correction, Empirical roughness model.

Claudio Frausto-Reyes Optics PhD, Transversal acoustic modes in resonant Raman: CdTe surface roughness study, Surface dependent behavior of CdS LO- phonon mode, Polarization dependent behavior of CdS around the first and second LO-phonon modes, Raman Spectroscopy, Mexican National Researcher, Reflectance equation correction, Empirical roughness model.

Juan Carlos Zenteno-Ruiz Medical Sciences PhD, Review and update on the molecular basis of Leber congenital amaurosis, Acro-spondylo-public dysostosis associated with cataracts, microcephaly, and normal intelligence, Gene therapy for hereditary ophthalmological diseases: advanced and future perspectives, Ophtalmogenetics, Mexican National Researcher, ocular genetics